Effects of Epidemiological Structure on the Transient Evolution of HIV Virulence

Sang Woo Park[1] Benjamin M. Bolker[1,2,3,*]

1 Department of Mathematics & Statistics, McMaster University, Hamilton, Ontario, Canada

2 Department of Biology, McMaster University, Hamilton, Ontario, Canada

3 Institute for Infectious Disease Research, McMaster University, Hamilton, Ontario, Canada

* bolker@mcmaster.ca

Abstract

The evolutionary dynamics of parasite virulence change in important ways over the course of an emerging epidemic. Changes in the fitness landscape generally select for higher virulence early in an epidemic; however, quantitative outcomes may depend sensitively on epidemiological details and the structure of mathematical models used to portray them. Fraser *et al.* have proposed a model for the eco-evolutionary dynamics of HIV that captures the tradeoffs between transmission and virulence (mediated by set-point viral load, SPVL) and their heritability between hosts. However, these models use implicit representations of the transmission process that drastically simplify the partnership dynamics that previous research has found to be critical in driving epidemics of sexually transmitted diseases. Our models combine HIV virulence tradeoffs with a range of epidemiological structures, modeling partnership formation and dissolution and allowing for individuals to transmit disease outside of partnerships. We assess summary statistics such as the peak virulence (corresponding to the minimum expected time of progression to AIDS) across all models for a range of partnership dynamic parameters applicable to the HIV epidemic in sub-Saharan Africa. Although

virulence trajectories are broadly similar across model structures, the timing and magnitude of the minimum expected time to progression vary considerably. Models of intermediate complexity as used by Shirreff *et al.* predicted lower slower progression/lower virulence (a minimum of 15 years to progress to AIDS) compared to both more realistic models and simple random-mixing models with no partnership structure at all (both with a minimum of ≈ 7.25 years to progress to AIDS). In this range of models, the simplest random-mixing structure best approximates the most realistic model; this surprising outcome occurs because the dominance of extra-pair contact in the realistic model tends to swamp the effects of partnership structure.

Author Summary

Pathogens such as HIV can evolve rapidly in response to changes in their environments; such changes include both increases in disease prevalence and disease virulence over the course of an epidemic, or decreases in both after treatment interventions. While researchers have successfully used computational models to explore these evolutionary dynamics, these models often neglect details such as the formation and dissolution of sexual partnerships; other research has shown that these processes can strongly affect epidemic outcomes. We built and compared models that used different methods to model both partnership dynamics and sexual contact outside of stable partnerships. Models of intermediate complexity predicted much lower virulence over the course of the epidemic (a minimum of 15 years to progress to AIDS) compared to both more realistic models and simple random-mixing models with no partnership structure at all (both approx. 7.25 years to progress to AIDS); sexual contact outside of stable partnerships tended to wash out the effects of epidemiological structure. The large differences in evolutionary dynamics among different epidemiological models suggests that researchers trying to predict the evolution of pathogens should proceed with caution.

Introduction

The evolution of pathogen virulence has both theoretical and, potentially, practical importance. In general, evolutionary theory suggests that disease strains that can

reproduce more — where reproduction is defined here as the amount of *between-host* transmission, or the number of new hosts infected — will increase in prevalence. Pathogens can increase their net reproduction rate either by increasing their transmission rate, the rate (per infected host) at which they infect new hosts, or by decreasing their clearance or disease-induced mortality rate, the rate at which hosts recover or die from disease. The *trade-off theory* [1] postulates that the transmission and disease-induced mortality rate are both linked to the rate at which the pathogen exploits host resources for within-host reproduction, and that pathogen evolution will thus strike a balance between the pathogen's rate of transmission to new hosts and its rate of killing its host (or of provoking the host's immune system to eliminate it). Some biologists have criticized the tradeoff theory [2,3], but others have successfully applied it to a variety of host-pathogen systems [4–7]. Fraser *et al.* have applied these ideas in a particularly interesting way by showing that HIV appears to satisfy the prerequisites of the tradeoff theory: in studies of discordant couples (i.e. long-term sexual partnerships with one infected and one uninfected partner), HIV virulence as measured by the rate of progression to AIDS was both heritable and covaried with the set-point viral load (SPVL: i.e., the characteristic virus load measured in blood during the intermediate stage of infection) and the probability of transmission. Higher viral loads led to shorter progression times (higher virulence) and faster transmission, with a decelerating relationship between virulence and transmission as required by the tradeoff theory [8,9]. Subsequent studies [10–12] used these data to parameterize mechanistic models of HIV virulence evolution, suggesting that HIV invading a novel population would initially evolve increased virulence, peaking after approximately 100-200 years and then declining slightly to a long-stable virulence level.

The work of Shirreff *et al.* [10], and particularly the predicted transient peak in HIV virulence midway through the epidemic, highlights the importance of interactions between epidemiological and evolutionary factors [13,14]. However, despite these studies' attention to detail at the individual or physiological level, the epidemiological structures used in these models are relatively simple.

As we discuss in detail below, existing models of HIV eco-evolutionary dynamics either use implicit models that incorporate the average effects of within-couple sexual contact — without representing the explicit dynamics of pair formation and dissolution

or accounting for extra-partnership contact — or use an agent-based formulation with parameters that effectively lead to random mixing among infected and uninfected individuals. Here we explore the effects of incorporating *explicit* epidemiological structure in eco-evolutionary models.

We add complexity to the epidemiological model following the general approach of Champredon *et al.* [15], which is in turn based on work of Dietz and Hadeler [16]; individuals join and leave partnerships at a specified rate, and can have sexual contact both within and outside of established partnerships. In order to explore how virulence evolution depends on epidemiological structure, we consider a series of models with increasing levels of complexity. In order to avoid dependence of the results on a particular set of parameters — as we explain below, finding matching sets of parameters across models with widely differing epidemiological structures is challenging — we evaluate our models across a wide range of parameters, again following Champredon *et al.* [15] in using a Latin hypercube design. For each model run, we compute a set of metrics (minimum progression time/peak virulence, timing of maximum virulence, equilibrium virulence) that summarize the evolutionary trajectory of a simulated HIV epidemic.

As our primary goal is to explore how different epidemiological structures (i.e. partnership dynamics and contact structures) affect our conclusions about the evolution of virulence, our models use a simplified description of within-host dynamics and heritability derived from Shirreff *et al.*'s multi-strain evolutionary model [10]. Like Shirreff *et al.*, we use a simple susceptible-infected-susceptible demographic formulation; rather than modeling birth and death (or more specifically, recruitment into the sexually active population and death), we assume that whenever an individual dies from infection, another enters the susceptible compartment.

Materials and Methods

Infection dynamics

As in Shirreff *et al.* [10], our models explicitly track the evolution of mean $\log_{10}$ SPVL (which we denote as α), rather than the rate of progression to AIDS itself (hereafter

"virulence" will refer either to the SPVL, or to the rate of progression to AIDS; these two quantities are deterministically linked in the model). In contrast to Shirreff *et al.*, we use a single-stage disease model instead of accounting explicitly for progression through the three main stages of HIV infection (primary, asymptomatic, and disease), and we use a simple exponentially distributed infectious period instead of a more realistic Weibull-distributed infectious period; we show below that our results are not overly sensitive to this simplification. We account for varying transmission rates and durations of each disease stage by summing the durations of three stages (again based on Shirreff *et al.*'s model) and taking the duration-weighted average of transmission rates of three stages. Thus the within-couple transmission rate, β, for our models is given by:

$$\beta(\alpha) = \frac{D_P\beta_P + D_A(\alpha)\beta_A(\alpha) + D_D\beta_D}{D_P + D_A(\alpha) + D_D}, \tag{1}$$

where the duration of infection (D_P and D_D) and rate of transmission (β_P and β_D) of the Primary and Disease stages of infection are independent of the host's SPVL. Following Shirreff *et al.*, the duration of infection (D_A) and rate of transmission (β_A) for the Asymptomatic stage are Hill functions of the SPVL:

$$\begin{aligned} D_A(\alpha) &= \frac{D_{\max} D_{50}^{D_k}}{V_\alpha^{D_k} + D_{50}^{D_k}}, \\ \beta_A(\alpha) &= \frac{\beta_{\max} V_\alpha^{\beta_k}}{V_\alpha^{\beta_k} + \beta_{50}^{\beta_k}}, \end{aligned} \tag{2}$$

where $V_\alpha = 10^\alpha$.

The uncoupled and extra-couple transmission rates (i.e., the rates of transmission among people outside of a stable partnership, or between people inside of a stable partnership and people other than their partner) are scaled by multiplying the within-couple transmission rate β by the contact ratios c_u/c_w and c_e/c_w (see Appendix S1). Simplifying the model of HIV pathogenesis from three stages to a single stage could affect our conclusions about the evolution of virulence (e.g. Kretzschmar and Dietz [17] show that pair formation dynamics and multiple stages of infectivity have interactive effects on $\mathcal{R}_0$). However, our simplified model produces results that are qualitatively similar to those of Shirreff *et al.*'s [10] model; when our model is calibrated to have a

similar initial epidemic growth rate r, the peak $\log_{10}$ SPVL occurs at the same time ($\approx$ 200 years) but slightly higher (4.6 $\log_{10}$ SPVL vs. 4.3 $\log_{10}$ SPVL, or 7% higher: Fig 1).

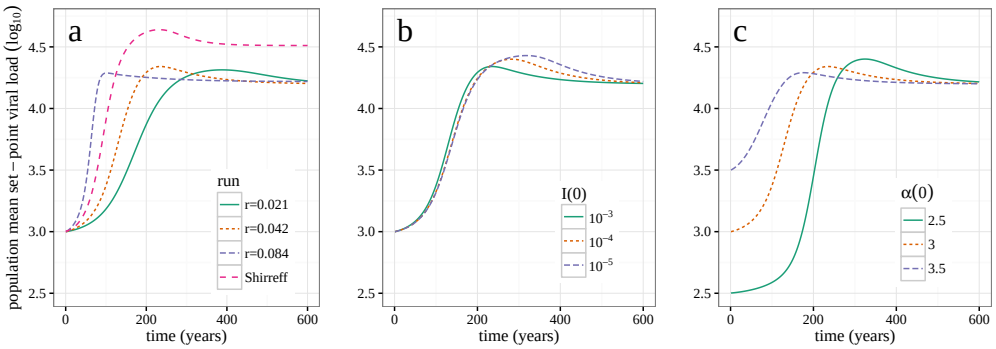

Fig 1. Baseline dynamics. Time series of mean population $\log_{10}$ SPVL. (a) Contrast between the three-stage Shirreff model and the single-stage model calibrated to varying initial exponential growth rates, r. (b) Effects of varying initial infectious density $I(0)$. (c) Effects of varying initial mean virulence $\alpha(0)$. The $r = 0.042$ (orange, dotted) curve in panel (a), calibrated to match the epidemic dynamics of Shirreff *et al.*'s model [10], shows that our simplified model can produce similar virulence trajectories. Panels b and c illustrate the sensitivity of virulence trajectories to initial conditions $I(0)$ and $\alpha(0)$, which we hold constant in our simulations.

Mutation

Like Shirreff *et al.* [10] we incorporate a between-host mutation process in the SPVL. We simplify Shirreff *et al.*'s evolutionary model by using a one-to-one genotype-phenotype mapping rather than allowing for variation in phenotypes of a single genotype. The mutational process in our model is directly taken from Shirreff *et al.*. Over the course of infection, mutation occurs within the host. However, it is assumed that SPVL of the strain transmitted by an infected individual is determined by the SPVL at the time of infection and is not further affected by within-host mutation. Instead, the mutational effect takes place in a single step at the time of transmission. First, the distribution of $\log_{10}$ SPVL is discretized into a vector:

$$\alpha_i = \alpha_{\min} + (\alpha_{\max} - \alpha_{\min})\frac{i-1}{n-1} \qquad i = 1, 2, 3, \ldots n. \tag{3}$$

We have experimented with varying degrees of discretization in the strain distribution (i.e., values of n); in our model runs comparing results with Shirreff *et al.* [10] (Fig 1) we use $n = 51$ (i.e. a bin width of 0.1 $\log_{10}$ SPVL for α), but reducing n to 21 (bin width

$= 0.25 \log_{10}$ SPVL) makes little difference; we use this coarser grid for all other simulations reported.

We construct an n by n mutational matrix, M — which is multiplied with the transmission term — so that M_{ij} is the probability that a newly infected individual will have $\log_{10}$ SPVL of α_j given that the infector has $\log_{10}$ SPVL of α_i. Finally, the probabilities are normalized so that each row sums to 1:

$$M_{ij} = \frac{\Phi(\alpha_j + d/2; i) - \Phi(\alpha_j - d/2; i)}{\Phi(\alpha_{\max} + d/2; i) - \Phi(\alpha_{\min} - d/2; i)}, \tag{4}$$

where $\Phi(x; i)$ is the Gaussian cumulative distribution function with mean α_i and variance of σ_M^2, and $d = (\alpha_{\max} - \alpha_{\min})/(n-1)$. Transmission rate and disease induced mortality rates are discretized as well:

$$\begin{aligned} \beta_i &= \beta(\alpha_i), \\ \lambda_i &= \frac{1}{D_P + D_A(\alpha_i) + D_D}. \end{aligned} \tag{5}$$

Contact structure and partnership dynamics

We developed seven multi-strain evolutionary models covering a gamut including Champredon *et al.*'s relatively realistic [15] and Shirreff *et al.*'s relatively simple [10] epidemiological structures, each of which is based on different assumptions regarding contact structure and partnership dynamics. Specifically, we focus on the effects of the assumptions of (1) instantaneous vs. non-instantaneous partnership formation; (2) zero vs. positive extra-partnership sexual contact and transmission; and (3) homogeneous vs. heterogeneous levels of sexual activity on the evolution of mean $\log_{10}$ SPVL.

Our first four models consider explicit partnership dynamics and are based on Champredon *et al.*'s model [15]. The first two ("pair-formation" or "pairform" for short) assume non-instantaneous partnership formation (i.e. individuals spend some time uncoupled, outside of partnerships) and consist of five states that are classified by infection status and partnership status. S is the number of single (uncoupled) susceptible individuals, and I is the number of single infected individuals. SS is the number of concordant negative (susceptible-susceptible) couples, SI is the number of serodiscordant (susceptible-infected) couples, and II is the number of concordant

positive (infected-infected) couples. The first ("pairform+epc") includes extra-partnership contact (with both uncoupled individuals and individuals in other partnerships) whereas the second ("pairform") only considers within-couple transmission.

The next two models, which are intended to bridge the gap between models with fully explicit pair-formation dynamics and the simpler, implicit models used by Shirreff *et al.* [10], assume instantaneous partnership formation ("instswitch"). The compartmental structure thus omits the single states S and I, comprising only the three partnered states: SS, SI, and II. Like the first two models, this pair of models differs in their inclusion of extra-pair contact: the third model ("instswitch+epc") includes extra-partnership contact (now only with individuals in other partnerships, since uncoupled individuals do not exist in this model) while the fourth ("instswitch") only considers within-couple transmission. Although these models can also be implemented by setting the partnership formation rate of the explicit partnership models to a high value (and we have tested that both methods in fact produce same results), we model instantaneous partnership formation models independently in order to avoid scaling of partnership formation rate during model calibration affecting the virulence trajectory.

The fifth and sixth models represent extreme simplifications of sexual partnership dynamics. One ("implicit") is an implicit serial monogamy model based on the epidemiological model used by Shirreff *et al.* [10]. It is actually a random mixing model that explicitly tracks only the total number of susceptible and infected individuals. However, to reflect the effect of partnership structure, it uses an adjusted transmission rate derived from an approximation of the basic reproduction number of a serial monogamy model with instantaneous pair formation [18]. The second model of this pair ("random") is a simple random-mixing model.

Lastly, we add a model of heterogeneity in sexual activity to the pairform+epc model ("hetero"). Individuals are divided into different risk groups based on the sexual activity level; we scale all aspects of sexual activity, assuming that sexual activity level in both within- and extra-couple contacts is directly proportional to number of non-cohabiting (extra-couple and uncoupled) partners per year [19] (see Appendix S1). We assume random activity-weighted mixing between risk groups [20]. While this model lacks some important elements, such as age-structured mixing patterns, needed for

realistic models of HIV transmission in sub-Saharan Africa, it represents a first step toward assessing the effects of epidemiological complexity. As even the models shown here push the limits of compartmental-based models (the heterogeneity model comprises 24530 coupled ordinary differential equations), adding further complexity will probably require a shift to an agent-based model framework, as well as considerable effort in model calibration [11, 21].

The pairform+epc and heterogeneous models use the basic epidemiological framework of Champredon *et al.* [15]. Individuals in single compartment acquire a partner at a rate ρ, and partnerships dissolve at a rate c. Infected individuals in a discordant partnership infect their susceptible partner at a rate β (within-couple transmission rate) and susceptible individuals outside the partnership at a rate c_e (extra-couple transmission rate). Likewise, a single infected individual can infect any susceptible individuals at a rate c_u through uncoupled mixing. Extra-couple and uncoupled transmission are modeled in the same way as in Champredon *et al.*'s model. All the details have been adapted to a multi-strain scenario, so that we track (for example) a matrix II_{ij} that records the number of concordant, HIV-positive couples in which the two partners have $\log_{10}$ SPVL of α_i and α_j. The second through fourth models (pairform, instswitch+epc, instswitch) are derived from the base model by simplifying epidemiological processes (partnership formation and uncoupled/extra-couple contact: see Appendix S1).

Latin hypercube sampling

Despite considerable effort [15, 18], the parameters determining the rate and structure of sexual partnership change and contact are still very uncertain; this led Champredon *et al.* [15] to adopt a Latin hypercube sampling (LHS) strategy [22] that evaluates model outcomes over a range of parameter values. In order to make sure that our comparisons among models apply across the entire space of reasonable parameter values, and in order to evaluate the differential sensitivity of different model structures to parameter values, we follow a similar protocol and perform LHS over a parameter set including both the early- and late-stage transmission and duration parameters (β_P, D_P, β_D, D_D) and contact/partnership parameters (ρ, c, c_u/c_w, and c_e/c_w). For the heterogeneity

model, the mean and squared coefficient of variation (CV) for the number of non-cohabiting partners are sampled as well. We do not allow for uncertainties in parameters that are directly related to the evolutionary process ($\beta_{\max}$, β_{50}, β_k, $D_{\max}$, D_{50}, D_k, σ_M), instead using Shirreff *et al.*'s point estimates throughout [10].

Latin hypercube sampling is done as in Champredon *et al.* [15]. For each parameter, z, its range is divided into $N = 1000$ equal intervals on a log scale:

$$z_i = \exp\left(\log(z_{\min}) + [\log(z_{\max}) - \log(z_{\min})]\frac{i-1}{N-1}\right) \qquad i = 1, 2, 3, \ldots, N. \qquad (6)$$

Random permutations of these vectors form columns in a sample parameter matrix; each row contains a different parameter set that is used for one simulation run.

Table 1 gives the ranges of the model parameters used for LHS. Parameter ranges regarding contact and partnership dynamics (ρ, c, and c_e/c_w) are taken from Champredon *et al.* [15], whereas those regarding infection (β_P, D_P, β_D, and D_D) are taken from Hollingsworth *et al.* [18]. The remaining parameters are taken from Shirreff *et al.* [10].

One parameter in our model, the ratio of uncoupled to within-couple transmission c_u/c_w, is needed to more flexibly contrast uncoupled and extra-couple transmission dynamics within multi-strain models (see Appendix S1); it appears neither in either Shirreff *et al.* nor Champredon *et al.*'s models, so we need to pick a reasonable range for it. Champredon *et al.* [15] assume that the effective within-couple contact rate and effective uncoupled contact rate have the same range of 0.05 - 0.25. Given Champredon *et al.*'s parameter range, the possible maximum and minimum values of c_u/c_w are 5 and 1/5. Therefore, we use 1/5-5 as the range for the parameter c_u/c_w. Although this adds more uncertainty to the parameter c_u — Champredon *et al.*'s range implies a 5-fold difference whereas ours gives a 25-fold difference — we consider the wider range appropriate, as little is not much known about the uncoupled transmission rate.

Two parameters, mean and the squared coefficient of variation (CV) of number of non-cohabiting partners, are sampled for heterogeneity in sexual activity. To allow for a wide range of uncertainty, range for the mean number of non-cohabiting partners was taken from unmarried men, as that was the group with the largest variability [19]. Omori *et al.* [19] give a very wide range for the coefficient of variation ($\approx$ 0 - 20,

Table 1. Parameter ranges/values. Values of c and ρ are doubled from those given by Champredon *et al.* because we keep track of individuals in the model, while they keep track of couples. Starred (*) parameters (used in Fig 1), and descriptions of Hill function coefficients, are taken from [10].

Notation	Description	Range/Value	Source
ρ	Partnership formation rate	1/10-2/5 per year	[15]
c	Partnership dissolution rate	1/15-1/5 (1.25*) per year	[15]
c_u/c_w	Relative contact rate for uncoupled transmission	1/5-5	Assumption
c_e/c_w	Relative contact rate extra-couple	0.01-1	[15]
β_P	Rate of transmission during primary infection	1.31-5.09 (2.76*) per year	[18]
β_D	Rate of transmission during high transmission disease stage	0.413-1.28 (0.76*) per year	[18]
D_P	Duration of primary infection	1.23/12-6/12 (0.25*) years	[18]
D_D	Duration of high transmission disease stage	4.81/12-14/12 (0.75*) years	[18]
$\beta_{\max}$	Maximum rate of transmission during asymptomatic stage	0.317 per year	[10]
β_{50}	SPVL at which infectiousness is half maximum	13938 copies per ml	[10]
β_k	Hill coefficient: steepness of increase in infectiousness as a function of SPVL	1.02	[10]
$D_{\max}$	Duration of primary infection	25.4 years	[10]
D_{50}	SPVL at which duration of asymptomatic infection is half maximum	3058 copies per ml	[10]
D_k	Hill coefficient: steepness of decrease in duration as a function of SPVL	0.41	[10]
σ_M	Mutation standard deviation of $\log_{10}$ SPVL	0.12	[10]
$\alpha_{\min}$	Minimum $\log_{10}$ SPVL	2	[10]
$\alpha_{\max}$	Maximum $\log_{10}$ SPVL	7	[10]
n	Number of strains	21 (51*)	Assumption
μ	Mean number of non-cohabiting sexual partners	0.103 - 1.206	[19]
κ	Squared coefficient of variation of number of non-cohabiting sexual partners	0.01 - 100	Assumption

corresponding to squared CV range of 0-400): we narrowed this range for CV^2 to 0.01-100. At the bottom end of the range, estimating that a group behaves perfectly homogeneously ($CV = 0$) is likely to be a sampling artifact; at the upper end, the estimate is also likely to be noisy because of the low mean value among married females (who have the largest range of CV). We assume that the number of non-cohabiting partners follows a Gamma distribution.

Simulation runs

One of the most difficult parts of model comparison is finding parameter sets that are commensurate with many different model structures. For the most part, our models are too complex to easily derive analytical correspondences among them. Given a numerical criterion, such as r (initial exponential growth rate) or $\mathcal{R}_0$ (intrinsic reproductive number), we can adjust one or more parameters by brute force to ensure that all of the models match according to that criterion. While $\mathcal{R}_0$ is often considered the most fundamental property of an epidemic, and might thus seem to be a natural matching criterion, here we focus on matching the initial growth rate r for several reasons. First, our primary interest is in the transient evolutionary dynamics of virulence, which are more strongly affected by r than $\mathcal{R}_0$. Second, r is more directly observable in real epidemics; r can be estimated by fitting an exponential curve to the initial incidence or prevalence curves [23], while $\mathcal{R}_0$ typically requires either (1) knowledge of *all* epidemic parameters or (2) calculations based on r and knowledge of the serial interval or generation interval of the disease [24]. Thus, we scale parameters so that every run has the same initial exponential growth rate in disease incidence.

In order to allow for all models to have equal initial exponential growth rate, r, we need to pick a parameter, s, such that $\lim_{s\to 0} r(s) = 0$ and $\lim_{s\to\infty} r(s) = \infty$. As adjusting either partnership change rate (i.e. partnership formation and dissolution rate) or transmission rate fails this requirement for some of our models, we scaled partnership change rate and dissolution rate by the same factor of γ: $\beta_{\text{adj}} = \gamma\beta_{\text{base}}$, $c_{\text{adj}} = \gamma c_{\text{base}}$, $\rho_{\text{adj}} = \gamma\rho_{\text{base}}$. Since transmission rate is adjusted by the scale of γ, uncoupled and extra-couple transmission rates are adjusted as well. For the instantaneous-switching and implicit models, none of which track single individuals, only the transmission rate and partnership dissolution rate (in this case equivalent to the partnership change rate) are adjusted.

We run each model for each of 1000 parameter sets chosen by Latin hypercube sampling, with fixed starting conditions of mean $\log_{10}$ SPVL of 3 and epidemic size of 10^{-4}. After each run, initial exponential growth rate is calculated. Then, parameters are scaled so that the initial exponential growth rate is scaled to 0.04, a value that approximates the growth rates of Shirreff *et al.*'s original models. For calibration

purposes, we run each model for only 500 years (full simulations are run for 4000 years), which is always long enough to capture the exponential growth phase of the model. We use a 4/5 order Runge-Kutta method (`ode45` from the `deSolve` package [25]) for all simulations. (For the heterogeneous model, approximately 10% of the samples failed due to numerical instability.)

Although each disease strain's core characteristic is its SPVL, the SPVL has one-to-one correspondences (based on eq. 2) with both the expected time to progression to AIDS and with the rate (probability per unit time) of HIV transmission. Because the time to progression (measured in years) is easier to interpret than SPVL (measured in $\log_{10}$ SPVL units), we summarize the virulence trajectories for each model run in terms of time to progression rather than SPVL. Because the time to progression is inversely related to SPVL (increasing SPVL decreases the time to progression), the time to progression is technically measuring inverse virulence rather than virulence (we did not think that reporting virulence as the rate of progression to AIDS, in units of years^{-1}, would help interpretability). For each model we derive the following summary statistics: minimum expected time to progression; time at which this minimum occurs (corresponding to peak virulence — this is also the time at which the maximum rate of progression, maximum SPVL, and maximum transmission rate occur); equilibrium time to progression; and the ratio of progression time at its minimum to the equilibrium value. Equilibrium progression time is calculated after 4000 years of simulated time. Although most simulations reach equilibrium much earlier, we set our time horizon at a much later date as some simulation runs have slow rate of evolution depending on the parameter set and model assumptions.

Knowing the minimum progression time, timing of the minimum progression time/peak virulence, and equilibrium progression time provide sufficient detail to identify the overall shape of the virulence trajectory. In particular, knowing the timing of the peak virulence (how many years into the epidemic the virulence peaks) can help epidemiologists guess whether the virulence of an emerging pathogen is likely (1) to have peaked early, possibly even before the pathogen is detected spreading in the population, and decline over the remaining course of the epidemic; (2) to increase, peak, and decline over the foreseeable future; or (3) to increase very slowly, peaking only in the far future. To the extent that our simplistic model for HIV reflects reality, we would

take the peak time of 150-300 years (Fig 1c) to mean that, in the absence of treatment, the epidemic would probably still be increasing in virulence.

Results

Our simplifications of Shirreff *et al.*'s model [10] reproduce its qualitative behaviour — in particular, its predictions of virulence dynamics — reasonably well. As r decreases from 0.084 to 0.42 (the latter value matching the initial rate of increase in prevalence in Shirreff *et al.*'s full model) the initial trajectory of increasing virulence brackets the rate from the original model (Fig 1a). However, our model produces lower peak virulence (≈ 4.3 vs. ≈ 4.6 $\log_{10}$ SPVL) and equilibrium virulence (≈ 4.25 vs. ≈ 4.5 $\log_{10}$ SPVL) than Shirreff's, even for matching initial incidence trajectories (i.e., $r = 0.042$ year^{-1}).

Changing the initial infectious density ($I(0)$), while it produces the expected changes in the initial epidemic trajectory (Supplementary material), has little effect on the virulence trajectory, making the virulence peaks slightly later and larger as $I(0)$ decreases. Decreasing $I(0)$ allows a longer epidemic phase before the transition to endemic dynamics (Fig 1b). Decreasing the initial virulence also leads to progressively later, larger peaks in virulence (Fig 1c).

Across the entire range of parameters covered by the LHS analysis, all of the classes of models we considered produce qualitatively similar virulence trajectories, which we quantify in terms of the expected time of progression to AIDS (Fig 2: lower progression time corresponds to higher virulence). Although the speed of virulence evolution varies, leading to wide variation in the minimum expected progression time (means ranging from approximately 6 to 12 years), virulence peaks in all models between 200 and 300 years.

Our chosen summary statistics (peak time, minimum expected progression time, equilibrium expected progression time, and relative progression time) all vary considerably across models (Fig 3). We first consider the models of intermediate realism: implicit, instantaneous-switching with and without extra-pair contact, and pair formation without extra-pair contact. Some parameter sets for these models lead to low equilibrium virulence (≈ 18 years to progression); these same sets lead to correspondingly low peak virulence (16 years to progression) and early peak times

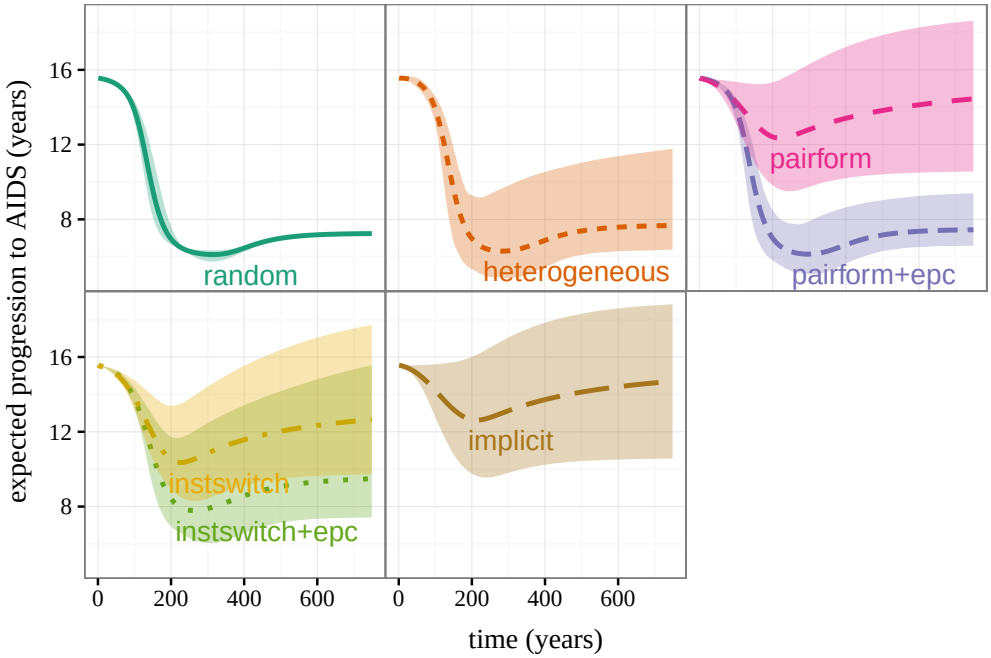

Fig 2. Envelopes of virulence trajectories (expected time of progression to AIDS) under all models. All models were run until $t = 4000$ years; truncated series are shown here.

(before 200 years: Fig 4). At the opposite extreme, parameter sets that produce high equilibrium virulence (8 years to progression) also produce late peaks (> 200 years) and high peak virulence (4 years to progression). The pair-formation without extra-pair contact and implicit models occasionally have parameter sets that select for such low virulence across the board that they never exceed their initial virulence, leading to a tail of peak times near zero.

The most striking aspect of the univariate comparisons in Fig 3, (and the bivariate comparisons in Fig 4) is the similarity between the results of the least (random mixing) and the most complex (pair formation with extra-pair contact, pairform+epc with heterogeneity) models. The random-mixing model has the lowest variability, because it is unaffected by uncertainty in pair formation and extra-pair contact parameters, but otherwise the virulence dynamics of these three extreme models are remarkably similar. This phenomenon is driven by the strong effects of extra-pair contact in the model with explicit pair formation and extra-pair contact ("pairform+epc" in Figs 2-5). When individuals spend time uncoupled between partnerships, and when these single individuals can transmit disease to coupled individuals, the resulting unstructured

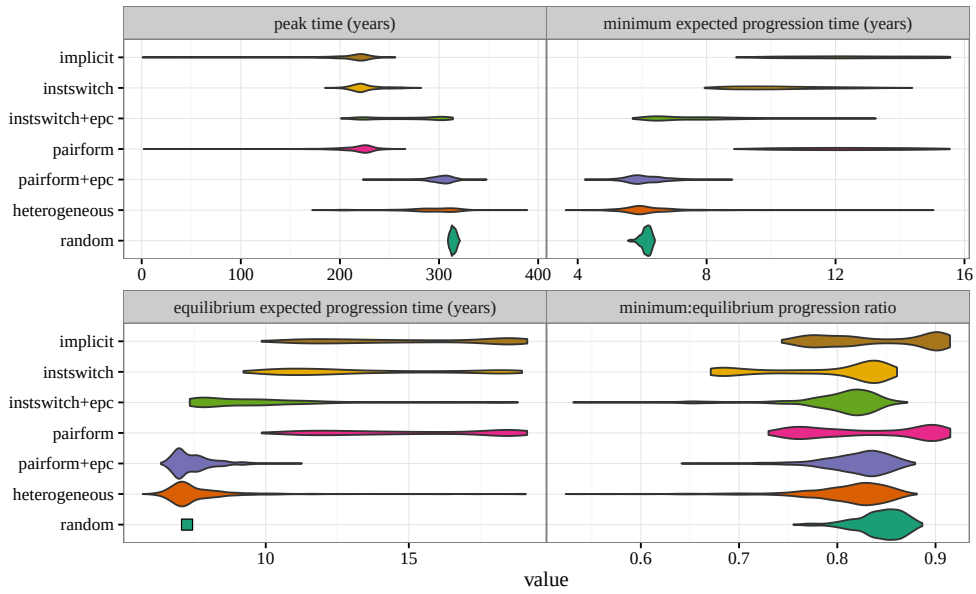

Fig 3. Univariate distributions of summary statistics. The distribution of equilibrium expected progression time (lower left panel) for the random mixing model is very narrow, and has been replaced by a point in order to preserve the vertical axis scaling.

mixing overwhelms the effect of structured mixing within couples, leading to mixing that is effectively close to random. Once unstructured mixing is strong, adding realistic heterogeneity of mixing to the model has little effect other than increasing the variability in the outcomes.

These differences are practically as well as scientifically important. The random-mixing, pairform+epc, and heterogeneous models all predict rapid progression to AIDS at the virulence peak (median/95% CI = 6.1 (5.7-6.3), 6.02 (5.04-7.7), 6.03 (4.8-9.2)). In contrast, the implicit model predicts minimum progression times about twice as long: 12.5 (9.6-15.6) years. The corresponding differences in within-couple transmission probability are even more extreme, about a fourfold difference: 0.249 (0.24-0.26), 0.252 (0.19-0.28), and 0.252 (0.15-0.28) per year for the random and pairform+epc models vs. 0.059 (0.02-0.13) per year for the implicit model (see Appendix S2 for plots showing univariate summaries of $\log_{10}$ SPVL and transmission probability).

The bivariate relationships (Fig 4) help distinguish the results of different models with similar univariate dynamical summaries. While the relationship between equilibrium progression time and peak time is similar for all model structures (top left panel), the other relationships show more variation. In particular, the implicit and

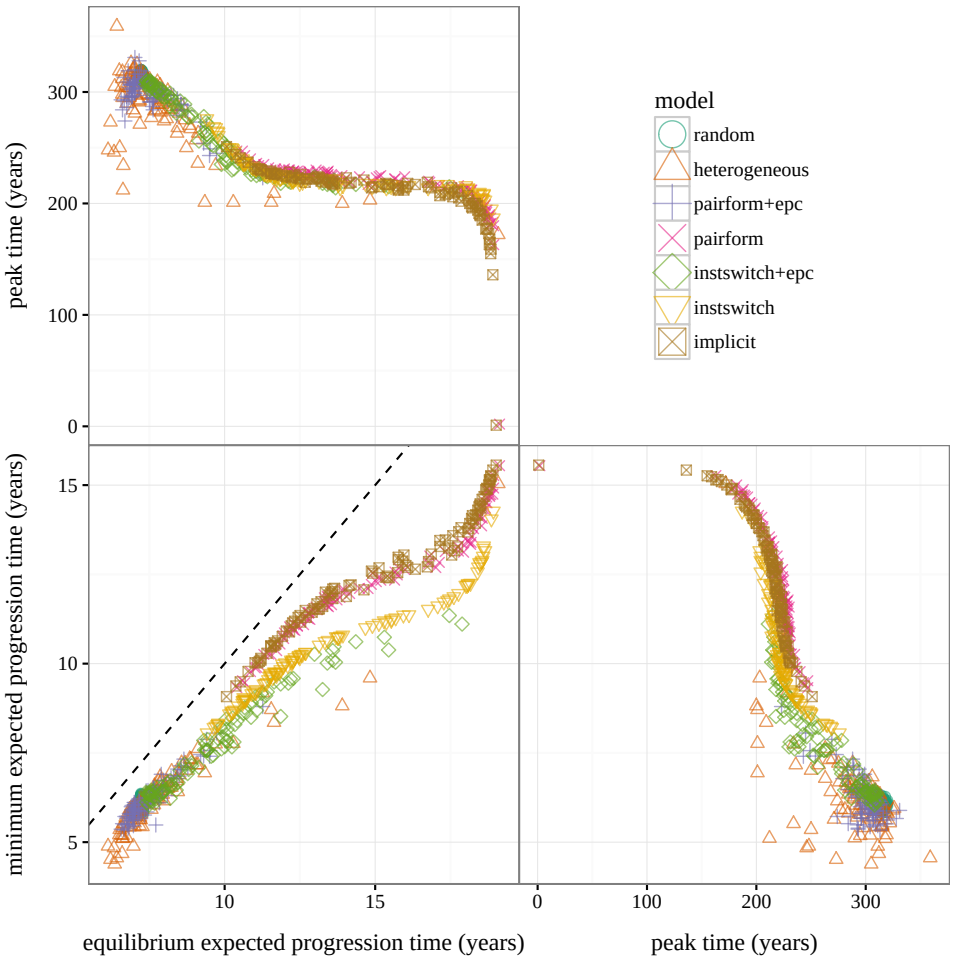

Fig 4. Pairs plot: bivariate relationships among summary statistics for each model structure. Dashed line in equilibrium vs. peak virulence plot shows 1:1 line. 100 values were sampled from each model to allow for clearer distinction between the models

pair-formation (without extra-pair contact) are very similar to each other, but distinct from the other models. We still do not have a convincing explanation for this distinction; we would have expected the implicit model to be most similar to the the instantaneous-switching model without extra-pair contact, which most closely matches its derivation. However, we note that the implicit model derivation is based on defining the force of infection to match a scaled version of $\mathcal{R}_0$, and as such would be expected to match the equilibrium behaviour but not necessarily the epidemic-phase behaviour of a model with explicit partnership dynamics.

Finally, the sensitivity plot (Fig 5) shows the effects of each parameter on the

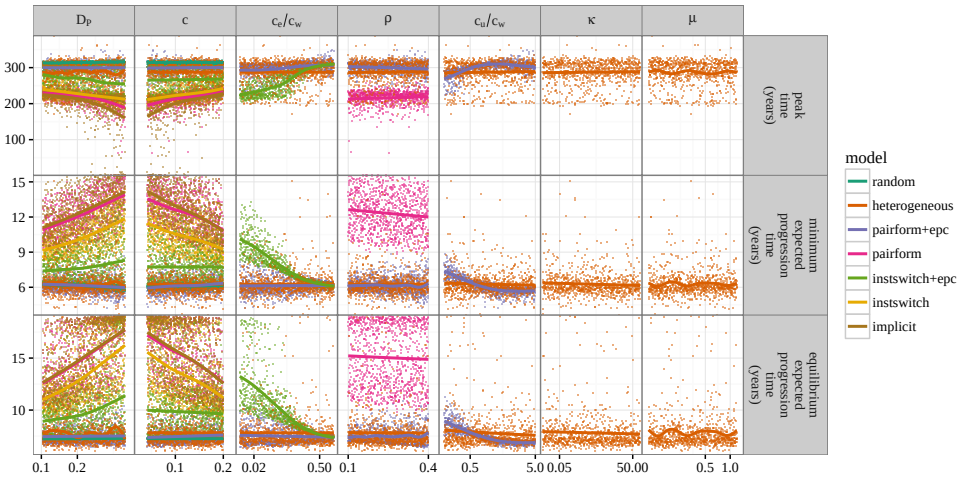

Fig 5. Sensitivity plot. For most parameters in the Latin hypercube sample and each summary statistic, the figure shows the distribution (points) and trend (smooth line) of the summary statistic as a function of the *unscaled* parameter value, i.e. prior to adjusting the parameters to achieve the standard initial epidemic growth rate.

summary statistics. In almost every case the effects of the parameters are monotonic; note that the plot shows the effects of the *unscaled* parameters, i.e. before they have been calibrated to achieve a standard initial epidemic growth rate. Increases in the transmission rates (β_P, β_D) and durations (D_P, D_D) in the primary and disease stages generally decrease the equilibrium virulence, peak virulence, and peak time, although the random and pair-formation+epc models have high, relatively constant values with respect to these parameters (because the patterns are so similar across this set of parameters, Fig 5 shows only D_P).

The partnership dissolution rate (c), which essentially acts as a contact rate in the model, increases virulence and peak time in almost all cases, although the pair-formation+epc model is again relatively insensitive. The ratio of extra-pair to within-pair contact (c_e/c_w) affects virulence in the instantaneous-switching+epc model, but not the pair-formation+epc model (probably because the uncoupled individuals present in the pair-formation+epc model make extra-pair contact by coupled individuals less important). Surprisingly, once calibration is taken into account, the remaining parameters have little effect overall. The rate of partnership formation (ρ) has little impact on the models with finite pair-formation times. The relative rate of uncoupled contact (c_u/c_w) slightly decreases the minimum and equilibrium progression time and delays the peak time in the pair-formation+epc model, but neither the uncoupled

contact rate nor the mean (μ) or CV^2 of the number of non-cohabiting sexual partners has much systematic effect in the heterogeneous model.

Discussion

All models must simplify the world. Many constraints — among them data availability, computation time, and code complexity — drive the need for parsimony, with different constraints applying in different contexts. The critical question that modelers must ask is whether the simplified model gives adequate answers, or whether the simplifications lead to qualitative or quantitative errors. This question is especially important for modelers who are hoping that their conclusions will guide management decisions.

In the particular example of HIV virulence eco-evolutionary dynamics and the complexity of epidemiological structures we reach the slightly ironic conclusion that the effort put into building a more realistic model essentially cancels out, putting us back where we started when used a naive random-mixing contact model. However, we are not quite back where we started, as the complex models lead to wider, presumably more realistic confidence intervals on the predictions. In general, unstructured mixing — whether occurring through purely random mixing, or through extra-pair contact and contact among people outside of stable partnerships — tends to drive faster virulence evolution, leading to higher peak virulence and lower times to progression at the peak time.

Taking further steps to make the model even more realistic might add further structure, making the random-mixing model predictions less accurate. For example, our model forms partnerships randomly, and assumes that extra-pair contact is randomly mixing across the population; one could instead model extra-pair contact as arising from multiple concurrent partnerships (some, such as contact with sex workers, of very short duration) and/or more structured partnership formation (by age, ethnicity, or behaviour group). The effects of other realistic complications such as explicit modeling of two sexes (both in contact structure and differential transmission probabilities), temporal and spatial variation in epidemic processes, or presence of genetic variation in hosts are harder to predict.

Parameterization is one of the biggest challenges of epidemiological modeling. In

addition to following Champredon *et al.* [15] by doing Latin hypercube sampling across a wide range of epidemiological parameters, we calibrated each set of parameters to the same initial epidemic growth rate, chosen to match the results of previous models [10]. Previous models in this area have drawn their parameters from cohort studies from the 1990s [18, 26] rather than doing any explicit calibration to epidemic curves, but they give reasonable order-of-magnitude growth rates (≈ 0.04 year^{-1}) for the early stages of the HIV epidemic (although considerably lower than estimates of $\approx 0.07 - 0.1$ year^{-1} based on population genetic reconstructions [27]). However, our reason for calibrating was not to match any specific observed epidemic, but rather to make sure that we were making meaningful comparisons across a range of models with radically different epidemiological structures, and hence involving different interpretations of the same quantitative parameters. For example, in models with instantaneous switching the partnership dissolution rate c is identical to the partnership formation rate; in models with explicit partnership formation, the partnership formation rate is also c at equilibrium, but might vary over the course of an epidemic. It is not obvious whether models with equal parameters but different structures should be directly compared; calibration solves this problem.

More generally, any model that wants to be taken seriously for management and forecasting purposes should be calibrated to *all* available data, using informative priors to incorporate both realistic distributions of uncertainty for all parameters from independent measurements [28] and calibration from population-level observations of epidemic trajectories. Such a procedure would also be an improvement on the common — although not universal — practice, which we have followed here, of assessing uncertainty over uniform ranges rather than using distributions that allow more continuous variation in support over the range of a parameter.

Researchers have documented that HIV virulence and set-point viral load are changing, on time scales comparable to those portrayed here (e.g., compare Fig 2 to Herbeck *et al.*'s estimated rate of change of 1.3 $\log_{10}$ SPVL per century [95% CI -0.1 to 3] [29]), and have begun to build relatively realistic models that attempt to describe how interventions such as mass antiretroviral therapy (ART) can be expected to change the trajectory of virulence evolution [30–32]. While these efforts are well-intentioned, we caution that epidemiological and other structural details that are currently omitted

from these models could significantly change their conclusions.

Acknowledgements

We would like to thank Christophe Fraser and David Champredon for access to simulation code; this work was funded by NSERC Discovery Grant 386590-2010.

Supporting Information

Appendix S1: model details

Appendix S2: dynamics of transmission and virulence

References

1. Alizon S, Hurford A, Mideo N, van Baalen M. Virulence evolution and the trade-off hypothesis: history, current state of affairs and the future. J Evol Biol. 2009;22:245–259. doi:10.1111/j.1420-9101.2008.01658.x.

2. Ebert D, Bull JJ. Challenging the trade-off model for the evolution of virulence: is virulence management feasible? Trends Microbiol. 2003;11(1):15–20.

3. Alizon S, Michalakis Y. Adaptive virulence evolution: the good old fitness-based approach. Trends in Ecology & Evolution. 2015;30(5):248–254. doi:10.1016/j.tree.2015.02.009.

4. Dwyer G, Levin SA, Buttel L. A simulation model of the population dynamics and evolution of myxomatosis. Ecol Monog. 1990;60:423–447.

5. Mackinnon MJ, Read AF. Genetic relationships between parasite virulence and transmission in the rodent malaria *Plasmodium chabaudi*. Evolution. 1999; p. 689–703.

6. Jensen KH, Little T, Skorping A, Ebert D. Empirical support for optimal virulence in a castrating parasite. PLoS Biol. 2006;4(7):e197.

7. De Roode JC, Yates AJ, Altizer S. Virulence-transmission trade-offs and population divergence in virulence in a naturally occurring butterfly parasite. Proceedings of the National Academy of Sciences. 2008;105(21):7489–7494.

8. Fraser C, Hollingsworth TD, Chapman R, de Wolf F, Hanage WP. Variation in HIV-1 set-point viral load: Epidemiological analysis and an evolutionary hypothesis. PNAS. 2007;104:17441–17446.

9. Fraser C, Lythgoe K, Leventhal GE, Shirreff G, Hollingsworth TD, Alizon S, et al. Virulence and Pathogenesis of HIV-1 Infection: An Evolutionary Perspective. Science. 2014;343(6177):1243727. doi:10.1126/science.1243727.

10. Shirreff G, Pellis L, Laeyendecker O, Fraser C. Transmission Selects for HIV-1 Strains of Intermediate Virulence: A Modelling Approach. PLoS Computational Biology. 2011;7(10):e1002185. doi:10.1371/journal.pcbi.1002185.

11. Herbeck JT, Mittler JE, Gottlieb GS, Mullins JI. An HIV Epidemic Model Based on Viral Load Dynamics: Value in Assessing Empirical Trends in HIV Virulence and Community Viral Load. PLoS Comput Biol. 2014;10(6):e1003673.

12. Herbeck JT, Mittler JE, Gottlieb GS, Goodreau SM, Murphy JT, Cori A, et al. Evolution of HIV virulence in response to widespread scale up of antiretroviral therapy: a modeling study. Virus Evolution. 2016;2(2):vew028. doi:10.1093/ve/vew028.

13. Day T, Proulx SR. A General Theory for the Evolutionary Dynamics of Virulence. The American Naturalist. 2004;163(4):E40–E63. doi:10.1086/382548.

14. Alizon S. The Price equation framework to study disease within-host evolution. Journal of Evolutionary Biology. 2009;22(5):1123–1132. doi:10.1111/j.1420-9101.2009.01726.x.

15. Champredon D, Bellan S, Dushoff J. HIV Sexual Transmission Is Predominantly Driven by Single Individuals Rather than Discordant Couples: A Model-Based Approach. PLoS ONE. 2013;8(12):e82906. doi:10.1371/journal.pone.0082906.

16. Dietz K, Hadeler KP. Epidemiological models for sexually transmitted diseases. Journal of Mathematical Biology. 1988;26(1):1–25.

17. Kretzschmar M, Dietz K. The effect of pair formation and variable infectivity on the spread of an infection without recovery. Mathematical Biosciences. 1998;148(1):83–113.

18. Hollingsworth TD, Anderson RM, Fraser C. HIV-1 Transmission, by Stage of Infection. Journal of Infectious Diseases. 2008;198(5):687–693. doi:10.1086/590501.

19. Omori R, Chemaitelly H, Abu-Raddad LJ. Dynamics of non-cohabiting sex partnering in sub-Saharan Africa: a modelling study with implications for HIV transmission. Sexually Transmitted Infections. 2015;doi:10.1136/sextrans-2014-051925.

20. May RM, Anderson RM. The Transmission Dynamics of Human Immunodeficiency Virus (HIV) [and Discussion]. Philosophical Transactions of

the Royal Society of London Series B, Biological Sciences. 1988;321(1207):565–607.

21. Delva W, Leventhal GE, Helleringer S. Connecting the dots: network data and models in HIV epidemiology. AIDS. 2016;30(13):2009–2020. doi:10.1097/QAD.0000000000001184.

22. Blower SM, Hartel D, Dowlatabadi H, Anderson RM, May RM. Drugs, Sex and HIV: A Mathematical Model for New York City. Philosophical Transactions of the Royal Society of London B: Biological Sciences. 1991;331(1260):171–187. doi:10.1098/rstb.1991.0006.

23. Ma J, Dushoff J, Bolker BM, Earn DJD. Estimating Initial Epidemic Growth Rates. Bulletin of Mathematical Biology. 2014;76(1):245–260. doi:10.1007/s11538-013-9918-2.

24. Wallinga J, Lipsitch M. How generation intervals shape the relationship between growth rates and reproductive numbers. Proceedings of the Royal Society of London B: Biological Sciences. 2007;274(1609):599–604. doi:10.1098/rspb.2006.3754.

25. Soetaert K, Petzoldt T, Setzer RW. Solving Differential Equations in R: Package deSolve. Journal of Statistical Software. 2010;33(9):1–25. doi:10.18637/jss.v033.i09.

26. Wawer MJ, Gray RH, Sewankambo NK, Serwadda D, Li X, Laeyendecker O, et al. Rates of HIV-1 transmission per coital act, by stage of HIV-1 infection, in Rakai, Uganda. Journal of Infectious Diseases. 2005;191(9):1403–1409.

27. Faria NR, Rambaut A, Suchard MA, Baele G, Bedford T, Ward MJ, et al. The early spread and epidemic ignition of HIV-1 in human populations. Science (New York, NY). 2014;346(6205):56–61. doi:10.1126/science.1256739.

28. Elderd BD, Dukic VM, Dwyer G. Uncertainty in predictions of disease spread and public health responses to bioterrorism and emerging diseases. Proceedings of the National Academy of Sciences. 2006;103(42):15693 –15697. doi:10.1073/pnas.0600816103.

29. Herbeck JT, Müller V, Maust BS, Ledergerber B, Torti C, Di Giambenedetto S, et al. Is the virulence of HIV changing? A meta-analysis of trends in prognostic markers of HIV disease progression and transmission. AIDS (London, England). 2012;26(2):193–205. doi:10.1097/QAD.0b013e32834db418.

30. Payne R, Muenchhoff M, Mann J, Roberts HE, Matthews P, Adland E, et al. Impact of HLA-driven HIV adaptation on virulence in populations of high HIV seroprevalence. Proceedings of the National Academy of Sciences. 2014;111(50):E5393–E5400. doi:10.1073/pnas.1413339111.

31. Roberts HE, Goulder PJ, McLean AR. The impact of antiretroviral therapy on population-level virulence evolution of HIV-1. Journal of The Royal Society Interface. 2015;12(113):20150888.

32. Herbeck J, Mittler J, Gottlieb G, Goodreau S, Murphy J, Cori A, et al. Evolution of HIV virulence in response to widespread scale up of antiretroviral therapy: a modeling study. bioRxiv. 2016; p. 039560.